Annals of Nuclear Energy 63 (2014) 751–762

Contents lists available at ScienceDirect

Annals of Nuclear Energy

journal homepage: www.elsevier.com/locate/anucene

Multi-group formulation of the temperature-dependent resonance scattering model and its impact on reactor core parameters

Shadi Z. Ghrayeb [a], Abderrafi M. Ougouag [b,*], Mohamed Ouisloumen [c], Kostadin N. Ivanov [a]

[a] Department of Mechanical and Nuclear Engineering, The Pennsylvania State University, 230 Reber Building, University Park, PA 16802, USA
[b] Idaho National Laboratory, MS-3860, PO Box 1625, Idaho Falls, Idaho 83415, USA
[c] Westinghouse Electric Company, 1000 Westinghouse Drive, Cranberry Township, PA 1606, USA

ARTICLE INFO

Article history:
Received 23 June 2013
Accepted 19 July 2013
Available online 11 October 2013

Keywords:
Resonance scattering
Multi-group formulation
Doppler effect
Up-scattering
Elastic scattering

ABSTRACT

A multi-group formulation for the exact neutron elastic scattering kernel is developed. It incorporates the neutron up-scattering effects stemming from lattice atoms thermal motion and it accounts for them within the resulting effective nuclear cross-section data. The effects pertain essentially to resonant scattering off of heavy nuclei. The formulation, implemented into a standalone code, produces effective nuclear scattering data that are then supplied directly into the DRAGON lattice physics code where the effects on Doppler reactivity and neutron flux are demonstrated. The correct accounting for the crystal lattice effects influences the estimated values for the probability of neutron absorption and scattering, which in turn affect the estimation of core reactivity and burnup characteristics. The results show an increase in values of Doppler temperature feedback coefficients up to −10% for UOX and MOX LWR fuels compared to the corresponding values derived using the traditional asymptotic elastic scattering kernel. This paper also summarizes research performed to date on this topic.

1. Introduction

The neutron slowing down equation,

$$\Sigma_t(E')\phi(E') = \int_0^\infty P(E \to E')\sigma_s(E)\phi(E)dE, \quad (1)$$

quantifies the balance of neutrons at energy E′ in an infinite domain, taking into account removal (the term on the left side of the equation) and slowing down into the energy E′, (integral term on the right side). In this equation, the slowing down term involves the scattering of neutrons from various initial energies into the energy E′, as represented by the differential scattering cross section,

$$\sigma_s(E \to E') = P(E \to E')\sigma_s(E).$$

This differential cross section is written as the product of a total scattering cross section (at energy E) and a transfer probability from E to E'. This probability inherently depends on the temperature of the scattering material. Yet, the common implementations of the solution of the neutron slowing down equation employ the temperature-independent "asymptotic scattering model" to describe the neutron-nucleus elastic scattering interactions. This "asymptotic" model, since independent of temperature, implicitly assumes that up-scattering events are ignored. Thus, in effect, rather than the equation shown above, the equation solved using traditional methods is

$$\Sigma_t(E')\phi(E') = \int_{E'}^{E'/\alpha} \frac{\sigma_s(E)}{(1-\alpha)E}\phi(E)dE. \quad (2)$$

This is tantamount to stating that the asymptotic kernel used to describe the elastic scattering transfer function is simply given by

$$\sigma_s(E)P(E \to E') = \begin{cases} \frac{\sigma_s(E)}{E(1-\alpha)}, & \alpha E \leqslant E' \leqslant E \\ 0, & otherwise \end{cases}, \quad (3)$$

where $\alpha = [(A-1)/(A+1)]^2$, in which A is the mass of the scattering nucleus in atomic mass units (amu). This scattering kernel explicitly states that neutrons starting at some energy E end with energy E' between E and αE, where α is positive and less than 1.0 and approaches zero when A is close to 1.0, i.e., when the scatterer is the nucleus of the lightest isotope of hydrogen.

The assumption of validity of the asymptotic model has been proved sufficiently accurate for neutrons scattering off of light isotopes but researchers who later questioned this theory have shown that the model is not quite as accurate for heavy nuclides with pronounced scattering resonances. The next section presents a brief review of historical developments on this subject and motivates the developments presented in this paper.

* Corresponding author. Tel.: +1 208 526 7659.
E-mail addresses: ghrays@gmail.com (S.Z. Ghrayeb), abderrafi.ougouag@inl.gov (A.M. Ougouag), ouislom@westinghouse.com (M. Ouisloumen), kni1@psu.edu (K.N. Ivanov).

0306-4549/$ - see front matter © 2013 Elsevier Ltd. All rights reserved.
http://dx.doi.org/10.1016/j.anucene.2013.07.031

2. A brief history of the resonance scattering model and recent developments

Until now, deterministic codes used to generate cross section data employed the asymptotic scattering model, which assumes the nucleus is at rest in the laboratory system. This assumption ignores any up-scattering events in the resonance domain. Wigner and Wilkins (1944) presented an integral equation describing the energy distribution of neutrons being slowed down uniformly throughout space by a uniformly distributed moderator whose atoms are in motion with a Maxwellian distribution of velocities. However, as they point out in their report, their formulation ignored the effects of chemical binding and crystal reflection. Blackshaw and Murray (1967) presented a new form of the scattering probability function in velocity space, assuming isotropic scattering in the center-of-mass system. In 1976, Cullen and Weisbin introduced the SIGMA1 kernel broadening method in which the cross sections are stored on a specific energy grid allowing for linear-linear interpolation between tabulated values (Cullen and Weisbin, 1976).

Ouisloumen and Sanchez (1990) first questioned the assumption made in the asymptotic scattering model (ASY) and derived a general expression (referred to here as the resonance scattering model – RSM) for temperature-dependent Legendre moments of the double differential elastic scattering cross section in a host medium characterized by a Maxwellian velocity distribution. Though their actual implementation of the model was limited to the zero-th order moment, it proved that the energy of a scattered neutron *can be* higher than the neutron energy prior to the scattering event in the resonance energy range – epithermal range. Their work also proved that the *average* neutron energy after the scattering event can be higher than the *average* energy predicted *post-event* by the asymptotic model. The same researchers also developed a Monte Carlo model and confirmed their own results (Ouisloumen, 1989). Their results revealed three important facts: (a) strong dependence of the shape of the transfer kernel on the resonance scattering cross-sections profile, i.e. the shape is far from being asymptotic when the initial neutron energy is in the vicinity of the resonance peak, particularly for the case of heavy nuclides, (b) the possibility of neutron up-scattering even at high energy, (c) strong dependence on the temperature of the scatterer target, i.e. fuel.

Later, other researchers (Kurchenkov and Laletin, 1991) proved the theoretical soundness of the model developed by Ouisloumen and Sanchez. In the mid-1990s Rothenstein and Dagan published a series of papers re-deriving the expression for the temperature-dependent transfer kernel and presenting their implementation using a stochastic methodology (Rothenstein and Dagan, 1995; Rothenstein 1996; Rothenstein and Dagan, 1998). Their papers provided a detailed explanation of the derivation of the resonance scattering model and its equivalence to the model developed by Ouisloumen and Sanchez.

In 2004, Rothenstein wrote a sequel to his previous papers, introducing a new formula to be integrated within code systems to enable the generation of $S(\alpha, \beta)$ tables (Rothenstein, 2004; Dagan, 2004). A year later in 2005 Dagan generalized the use of $S(\alpha, \beta)$ tables for ^{238}U (Dagan, 2005) and then later applied them to a burnup PWR application and reported as much as a 660 pcm change over a burnup cycle and an increase in ^{239}Pu production (Dagan and Broeders, 2006). The same method was later applied by Becker et al., 2008; Becker et al., 2009a, using MCNP (X-5 Monte Carlo Team, 2003) by preparing new $S(\alpha, \beta)$ scattering law tables and applying them to high temperature reactor (HTR) pin- and full-core calculations. They compared the use of the new scattering kernel with MCNP's standard approach ("Sampling of Velocity of Target nucleus" – SVT – which assumes the microscopic elastic scattering cross section is constant) and reported an increase in Doppler reactivity coefficient by 10% for the HTR-10 unit cells (Becker et al., 2009a), a decrease in criticality of 170–600 pcm depending on TRISO packing fraction and fuel temperature and an increase of up to 2.5% of ^{239}Pu production at end of cycle for fuel burnup. At the full-core level the same authors report a more negative Doppler reactivity by 14% and a decrease of the effective multiplication by 200–400 pcm for a model representative of the HTTR design (Becker et al., 2009a). In the same year, Becker et al. (2009b) introduced an improved Doppler broadened rejection correction (DBRC) (Becker, 2010) approach and used it to replace the approximation incorporated in MCNP concerning the scattering kernel in the resolved resonance range of heavy nuclei. The improved DBRC approach matched the results of the $S(\alpha, \beta)$ tables for heavy nuclides (presented by Dagan in 2005) to within 1–2 standard deviations with the DBRC approach increasing computation time by as much as 20%. The Doppler coefficient for their UOX fuel pin-cell model (4 $^{w}/_{o}$ ^{235}U) differed by as much as 16% when compared to the MCNP standard scattering kernel (fuel temperature range between 800 K and 1200 K). Further work by Becker et al. (2009c) applied the same methods just discussed to the Mosteller benchmark (Mosteller, 2006; Mosteller, 2007) for UOX and MOX fuel, reporting a difference of 8–16% in Doppler coefficient when compared to results obtained with the standard MCNP kernel. Likewise, when applied to a CANDU-6 model the DBRC method results in a slightly more negative fuel temperate coefficient (Dagan et al., 2011a). All the results reported by Dagan and Becker et al. were limited by applying the resonance scattering kernel only for ^{238}U and covering the energy range 10^{-5}–210 eV, thus ignoring potential effects from other nuclides and at energies outside that range.

At the same time as Becker et al. presented their results, Lee et al. (2008, 2009) applied the resonance scattering effects (via Weight Correction Method – WCM) for ^{238}U scattering data. They used Monte Carlo methods to generate the resonance integral data for CASMO-5 (Rhodes et al., 2006) and applied it to the UOX Mosteller benchmark case. Their results report a more negative fuel temperature coefficient of 9–10% (depending on the ^{235}U $^{w}/_{o}$ enrichment) and lower eigenvalues by as much as 212 pcm when compared to the asymptotic model. In the case of a HTR fuel the same researchers report a decrease in reactivity equivalent to $\sim$−450 pcm (at 1350 °C). Their results were limited to applying the resonance scattering kernel only for the ^{238}U nuclear data covering energy ranges with an upper limit of 1000 eV. The effect of the resonance scattering model and its influence on LWR reactivity initiation accidents was also studied (Grandi et al., 2010).

Likewise, later in 2009 Mori and Nagaya implemented the corrected resonance scattering model in the Monte Carlo code MVP-2 (Nagaya et al., 2005) and also applied it to the UOX Mosteller benchmark (Mori and Nagaya, 2009). They report more negative Doppler reactivity coefficients by 7.2(±0.1) to 11.7±(0.2)% (depending on the ^{235}U $^{w}/_{o}$ enrichment) when compared to the asymptotic model. Their studies included applying the corrected scattering model for energies greater than 4.5 eV and unlike previous calculations by others, applied the model to ^{238}U and ^{235}U nuclei. In 2012, Kim and Hartanto used the modified MCNP code, using Becker's DBRC method, and analyzed the fuel burnup, fuel temperature coefficient and power coefficient of reactivity for CANDU-6 (Kim and Hartanto, 2012). Zoia et al. included the DBRC and WCM techniques in the TRIPOLI-4 code, applying it to the UOX and MOX Mosteller benchmarks and performed depletions studies (Zoia et al., 2013). Hart et al. also updated the KENO Monte Carlo code, within the SCALE code system (RSICC Computer Code Collection, 2011), to include the DBRC technique (Hart et al, 2013). Further work included a burnup study (based on the DBRC technique) for

UOX and MOX pin-cell depletion, applying the resonance scattering model for all uranium and plutonium isotopes (Trumbull and Fieno, 2013) using the Monte Carlo code MC21 (Sutton et al., 2007).

Later work by the present authors (Ghrayb et al., 2010a; Ghrayeb et al., 2010b; Ghrayeb et al., 2011a; Ghrayeb et al., 2011b) and subsequently by others (Arbanas et al., 2011; Arbanas et al., 2012; Sunny and Martin, 2013), extended the original formulation to incorporate anisotropic terms of the angular distribution expansion in Legendre polynomials. Recently, Sanchez and coworkers (Sanchez et al., 2013) again implemented the original resonance scattering model in the APOLLO2 code (Sanchez et al., 1988), i.e., assumed only isotropic scattering, but used faster computational schemes.

In 2012, Sunny et al. performed similar work to that of Becker et al. but modified the DBRC method with a revised rejection scheme, implementing it in MCNP, and applying it to the UOX Mosteller benchmark. Their results also indicate a more negative temperature coefficient (Sunny et al, 2012) but with a difference ranging from 4.2(±0.3) to 15.2(±1.0)% (depending on ^{235}U $^{w}/_{o}$ enrichment), which extends beyond the range reported by Lee et al. 2009; Mori and Nagaya, 2009 and Ghrayeb, 2013. Furthermore, their results were limited to applying the resonance scattering model to ^{238}U only and for energies with an upper limit of 210 eV.

Limited work has been performed introducing the resonance scattering formulation and its implementation using a deterministic approach. In 1994, Bouland et al. performed calculations with RSM being applied to ^{238}U for a UOX fueled pin-cell (^{235}U enrichment not specified) and stated that one "expects the thermal reactor Doppler effect to increase by about 9%", compared to the asymptotic kernel, and a rise in resonance absorption rate to about 1% at reactor operating temperatures (Bouland et al., 1994). Their model was applied to the energy range 6.16–454 eV. A study was published in 2006 by Kolesov and Ukraintsev modeling the resonance scattering model in a standalone slowing down code and evaluating its effects on simple pin-cells with different moderator-to-fuel volume ratios (Kolesov and Ukrainstev, 2006). In 2010, Peng et al. implemented the resonance scattering model for the slowing down equation in the numerical program Estuary but did not apply it to any pin-cell models (Peng et al., 2010). Oberle implemented the corrected resonance scattering kernel and reported a negative Doppler coefficient increase of 9% for PWR reactor core simulations (Oberle, 2010). In 2012, Ono et al. reported applying the resonance scattering model for heavy nuclides, but approximated the up-scattering term using the narrow resonance (NR) approximation (Ono et al., 2012). They implemented their model in the GROUPR module of NJOY (MacFarlane and Muir, 2000) then applied their calculations to the Mosteller benchmark for UOX fuel finding a difference in the Doppler coefficient of 9.3–10.1% when compared to the asymptotic scattering kernel. Their MOX Mosteller calculations show a Doppler difference of 6.2–7.2%. They had applied the resonance scattering kernel for ^{238}U, ^{239}Pu and ^{240}Pu over the range of 4–200 eV. As seen later, the present paper, for the first time, extends the resonance scattering model to a fully multi-group implementation and reports a difference in Doppler coefficient of 8.6–9.8%, when compared to the asymptotic scattering model for the UOX Mosteller benchmark and 6.9–9.8% for the MOX benchmark. These results include applying the corrected model for all heavy nuclides (actinides) and over the entire energy spectrum (upper limit of 20 MeV). The details of these new developments and of these latter results are presented in this current paper. Table 1 summarizes all work performed to-date relating to applying the corrected resonance scattering model to the Mosteller benchmark. Further discussions concerning all previous results on application of the RSM to the Mosteller benchmark are presented in the conclusion section of this paper (figure in that section and related text).

Questions were raised concerning the approximation of treating the velocity distribution of the target nucleus as that of atoms in a free gas (Maxwellian distribution) and about whether the effect of lattice vibrations on nuclear resonances is accurately accounted for (Hove, 1954; Word and Trammell, 1981; Cuello and Granada, 1997; Meister and Santamarina, 1998; Naberejnev et al., 1999; Dagan et al., 2007; Naberejnev, 2001). Lamb (1939) suggested that in the case of a weak lattice binding it is possible to treat bound atoms as if they were in a gas. Courcelle and Rowlands (2007) simulated resonance scattering using solid-state effects and concluded that relatively small differences arose when compared to results using the treatment by the resonant free gas scattering kernel model. In addition, experimental work carried out at the Rensselaer Polytechnic Institute's linear accelerator provided data validating the improved free gas model (Danon et al., 2009; Ro et al., 2009; Dagan et al, 2011b).

Most implementations by other researchers thus far were limited to the Monte Carlo approach. The current paper introduces a formulation and implementation that are fully compatible with deterministic codes, both for the zero-th order and higher order terms. The prior implementations discussed above are limited either in the energy range to which the resonance scattering model was applied or in their implementation for only selected heavy nuclides. The present paper is first to extend the previous approaches to a fully multi-group formulation and to demonstrate the implementation of the new formulation into an existing deterministic lattice physics code. Preliminary results from this multi-group formulation have been presented at conferences (Ghrayeb et al., 2011c Ghrayeb et al., 2012). The present paper reports on implementing the RSM to elastic cross-section data in the DRAGON deterministic lattice physics code. A very fine energy group structure is devised for this purpose. The method is applied to the Mosteller benchmark, thus demonstrating the RSM effects on the Doppler coefficient of reactivity and on the neutron flux. The results for UOX and MOX fuel pin-cell calculations incorporating temperature- and velocity-dependent cross sections, using the corrected scattering kernel, are presented.

3. Formulation

The exact form of the n-th Legendre moment of the differential elastic scattering cross-section for lattice interactions in which energy may be either lost or gained by the neutron, originally derived by (Ouisloumen and Sanchez, 1990) states

$$\sigma_{sn}^{T}(E \to E') = \frac{\beta^{\frac{5}{2}}}{4E} e^{\frac{E}{kT}} \int_0^\infty t\sigma_s^{tab}\left(\frac{\beta kT}{A}t^2\right) e^{-\frac{t^2}{A}} \Psi_n(t)dt. \quad (4)$$

In this equation, t is a variable proportional to the neutron-nucleus relative speed, β is the ratio $\frac{A+1}{A}$, where A is the atomic mass of lattice atoms expressed in amu (i.e., the ratio of the lattice nucleus mass to the mass of the neutron), k is Boltzmann's constant, σ_s^{tab} stands for the tabulated cross-section values at the temperature of 0 K, and T designates the temperature of the lattice. The function $\Psi_n(t)$ is the nth order component of the angular dependence of the scattering kernel. An explicit mathematical expression for $\Psi_n(t)$ was originally derived by Ouisloumen and Sanchez and is reproduced in Ghrayeb et al. (Ghrayeb et al., 2011b) for completeness, with corrections.

In this paper only isotropic scattering (i.e., $\Psi_0(t)$, the 0th angular moment component) is considered for the multi-group formulation. Starting from Eq. (4), the multi-group matrix is obtained using a double integral,

Table 1
Summary of results performed using the resonance scattering model applied to the Mosteller benchmark.

#	Researcher(s)	Energy range	Nuclei	Method	CODE	LIBRARY	Fuel	Δk (pcm)	FTC diff. (%)[1]
1	Becker et al., 2009c	<210 eV	^{238}U	SVT vs. DBRC	MCNP5	JEFF3.1	UOX	–	8–16[2]
				SVT vs. DBRC			MOX[a]		
				SVT vs. DBRC			MOX[b]		
2	Sunny et al., 2012	<210 eV	^{238}U	DBRC	MCNP5	ENDF/B-VII	UOX	6 ± 25–194 ± 40	4.2 ± 0.3–15.2 ± 1.0
3	Sunny 2013	<210 eV	^{238}U	DBRC	MCNP5	ENDF/B-VII	UOX	20 ± 40–271 ± 41	8.8 ± 0.6–25.1 ± 1.7
4	Mori and Nagaya, 2009	>4.5 eV	^{238}U, ^{235}U	ASY vs. WCM	MVP-2	JENDL-3.3	UOX	72 ± 8–222 ± 14	7.2 ± 0.1–11.7 ± 0.2
5	Zoia et al., 2013	<210 eV	^{238}U	SVT vs. DBRC	TRIPOLI-4	ENDF/B-VII	UOX	66 ± 13–225 ± 14	6.2 ± 0.2–12.8 ± 0.3
6		<210 eV	^{238}U	SVT vs. WCM		ENDF/B-VII	UOX	77 ± 13–274 ± 18	8.7 ± 0.2–15.6 ± 0.4
7		0.1 eV–1 keV	^{238}U	SVT vs. DBRC		CEAV5.1	UOX	59 ± 6–232 ± 7	9.6 ± 0.1–12.7 ± 0.2
8		0.1 eV–1 keV	All nuclei	SVT vs. DBRC		CEAV5.1	UOX	62 ± 6–233 ± 7	9.3 ± 0.1–12.4 ± 0.1
9		0.1 eV–1 keV	^{238}U	SVT vs. DBRC		CEAV5.1	MOX[a]	67 ± 7–177 ± 6	7.0 ± 0.1–9.1 ± 0.1
10		0.1 eV–1 keV	All nuclei	SVT vs. DBRC		CEAV5.1	MOX[a]	108 ± 7–222 ± 6	8.0 ± 0.1–11.2 ± 0.1
11		0.1 eV–1 keV	Actinides	SVT vs. DBRC		CEAV5.1	MOX[a]	113 ± 7–232 ± 6	7.5 ± 0.1–11 ± 0.1
12	Ono et al., 2012	4–200 eV	Not specified	Deterministic	Not specified	Not specified	UOX	50–200	9.3–10.1[3]
13		4–200 eV					MOX[a]	70–160	6.5–7.2[4]
14	Lee et al., 2009	<1000 eV	^{238}U	ASY vs. WCM	CASMO-5[5]	ENDF/B-VII	UOX	59–212	9.2–9.8
15	Ghrayeb et al.	<20 MeV	Actinides	Deterministic	DRAGON	ENDF/B-VII	UOX	68–208	8.6–9.8
16	(current work)	<20 MeV	^{238}U				UOX	68–205	8.6–9.7
17		<20 MeV	^{238}U				MOX[a]	74–165	6.2–7.9
18		<20 MeV	Actinides				MOX[a]	115–216	7.5–8.7
19		<20 MeV	^{238}U				MOX[b]	89–187	6.9–9.6
20		<20 MeV	Actinides				MOX[b]	109–218	7.7–9.8

[1] FTC Diff.(%) $= \frac{FTC_{ASY} - FTC_{RSM}}{FTC_{ASY}} \times 100$, see Eq. (8) for FTC.
[2] The FTC differences for each enrichment case were not individually documented.
[3] The difference in the Doppler reactivity coefficient were calculated manually and vary from the numbers reported in their paper.
[4] Based on Pu_2O_2 content of 4 wt.%, and 8 wt.% (their 20 wt.% cases was excluded due to a typo in their paper).
[5] The resonance integral data was calculated using their Monte Carlo Slowing Down code: MCSD code and supplied to CASMO-5.
[a] Reactor-Recycle MOX fuel.
[b] Weapons-Grade MOX fuel.

$$\sigma_{s0}^{Tg\to g'} = \frac{1}{\delta_g \delta'_g} \int_{E_g}^{E_{g+1}} dE \int_{E_{g'}}^{E_{g'+1}} dE' \sigma_{s0}^{T}(E \to E') \tag{5}$$

where $\delta_g = E_{g+1} - E_g$, with a similar expression applying for $\delta_{g'}$ The above equation applies to all cases (down-scattering, up-scattering and within-same-group scattering). However, for the within-group scattering case it is advantageous to reformulate the equation in a way that makes more convenient the explicit use of different expressions for the up- and down-scattering kernels. The equation, in the case of within-group scattering, is best written as

$$\sigma_{s0}^{Tg\to g} = \frac{1}{\delta_g \delta_g} \times \int_{E_g}^{E_{g+1}} dE \left\{ \int_{E_g}^{E} dE' \sigma_{s0}^{T}(E \to E') + \int_{E}^{E_{g+1}} dE' \sigma_{s0}^{T}(E \to E') \right\} \tag{6}$$

It is understood that in the above equation the scattering moment assumes different forms that depend on the modeled situation being an up-scattering event or a down-scattering one.

Eqs. (5) and (6) are evaluated numerically using Gauss-Legendre quadratures. In the course of data preparation (i.e., application of Eq. (4)), the correction of the scattering kernel was performed over the entire neutron energy spectrum for each heavy isotope so that all the scattering resonances were correctly treated. More detailed explanations of the calculations performed in this paper can be found in (Ghrayeb, 2013).

For verification purposes, regarding the data preparation phase, the multi-group results obtained in this paper are compared to the corresponding analytic (i.e., continuous energy) values reported in (Ghrayeb et al., 2011b). Regarding the application to reactor physics situations, the verification is carried out in comparisons of results obtained by other authors. Specifically, the results obtained using the corrected scattering kernels in the deterministic calculation of this work are compared with the results of (Lee et al., 2009) who implemented Monte Carlo versions of the corrected scattering kernel method into CASMO-5.

4. Results

Some of the tests used to verify the implementation of the multi-group form of the scattering kernels model are presented here. The test implementation shown here uses thin energy groups ($\delta_g < 10^{-3} eV$) in order to approach the analytic values in the sense that when the energy group width is refined, the group cross section approaches the value of the continuous energy cross section at mid-group. In symbols,

$$\delta_g \to 0, \delta_{g'} \to 0 \Rightarrow \sigma_{s0}^{Tg\to g'} \sim \sigma_{s0}^{T}(\bar{E}_g \to \bar{E}_{g'});$$

$$\bar{E}_g = \frac{E_{g+1} + E_g}{2}, \quad \frac{E_{g'+1} + E_{g'}}{2}.$$

Numerical integration of Eqs. (5) and (6) is carried out to compute the multi-group scattering matrix. The calculations are compared, for accuracy, to the results produced by the analytic values documented in (Ghrayeb et al., 2011b) and partially reproduced here. Neutrons were started at various energies and temperatures and the corresponding scattering kernels were computed. Fig. 1 displays the analytic and multi-group scattering transfer kernels for a temperature of 1000 K, starting at an energy of 6.52 eV, just below the first resonance of ^{238}U (6.67 eV). In this model neutrons are assumed to be present at the "starting" energy and the computation evaluates their energy change as caused by scattering. In the case of the neutrons described above with a starting energy just below the resonance, a significant amount of up-scattering is displayed in the figure. The results in Fig. 1 clearly show the agreement between the analytic (continuous energy) and multi-group results. Likewise, neutron energies started at 659.05 eV also show good agreement, as displayed in Fig. 2.

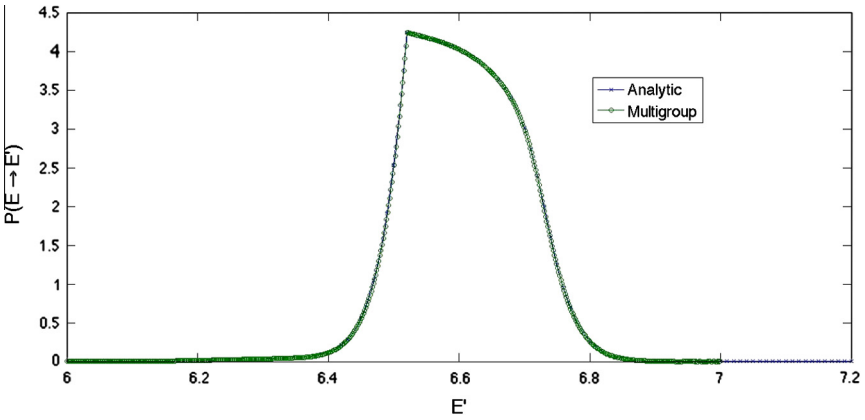

Fig. 1. Scattering kernel of ^{238}U at 1000 K for neutron starting at energy 6.52 eV.

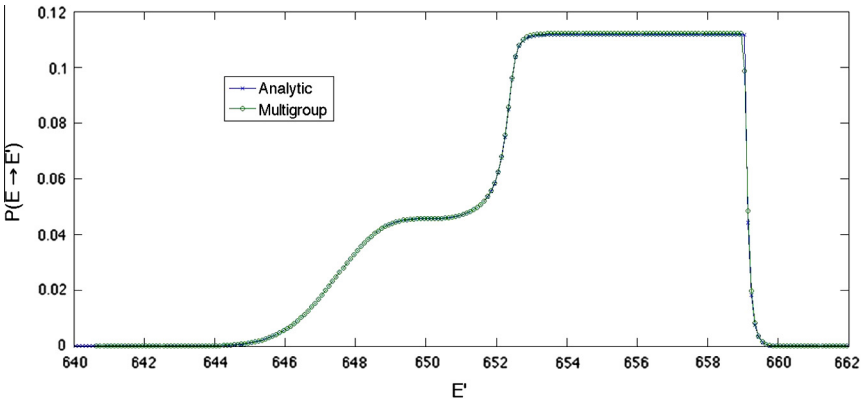

Fig. 2. Scattering kernel of ^{238}U at 1000 K for neutron starting energy of 659.05 eV.

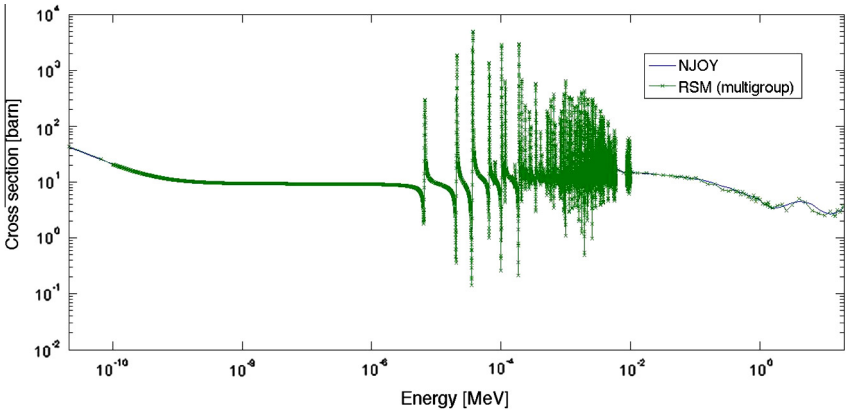

Fig. 3. The elastic cross section for ^{238}U at 900 K comparing NJOY multi-group results with those of the RSM using the same energy group structure.

An additional verification is achieved by comparing the total scattering cross section in group g of the multi-group matrix with the corresponding cross section as generated using NJOY.[1] This comparison is carried out by first computing the total scattering cross section in group g as a summation of the group to group cross section over all final energy groups. Thus, the total cross-section is given by

$$\sigma_{s0}^{Tg} = \sum_{g'=1}^{N_g} \delta_{g'} \sigma_{s0}^{Tg\to g'}, \tag{7}$$

where all variables were defined earlier. The quantity on the left of Eq. (7) is computed directly with NJOY, using the GROUPR module; while the right side is computed from the values generated using the RSM standalone code. A comparison provides proof of correctness of the multi-group implementation of the RSM when the two sides of Eq. (7) thus obtained are indeed equal. This is the case because the transfer probability is normalized to one, hence the

[1] In this paper, whenever the NJOY code is mentioned, it is implicit that version 99.364 is meant.

Table 2
Fuel temperature coefficients for the Mosteller UOX benchmark with uranium enrichments ranging from 0.711% to 5.0% and the RSM kernel applied only to ^{238}U.

wt (%)	k (asymptotic kernel)			k (RSM kernel only for ^{238}U)			FTC diff (%)
	HZP	HFP	FTC	HZP	HFP	FTC	
0.711	0.6621394	0.6560206	−4.70	0.6614598	0.6548324	−5.10	−8.62
1.6	0.9562254	0.9478355	−3.09	0.9553188	0.9461777	−3.37	−9.25
2.4	1.0939660	1.0847290	−2.59	1.0929660	1.0828760	−2.84	−9.52
3.1	1.1716930	1.1620540	−2.36	1.1706490	1.1601060	−2.59	−9.66
3.9	1.2341210	1.2242040	−2.19	1.2330470	1.2221950	−2.40	−9.70
4.5	1.2694110	1.2593600	−2.10	1.2683240	1.2573230	−2.30	−9.72
5.0	1.2936360	1.2835050	−2.03	1.2925430	1.2814540	−2.23	−9.72

integral of the scattering cross section (including the transfer kernel factor) over all final energy values works out to the elastic cross section for the initial group, g, the very quantity directly computed when using NJOY. The result of the comparison is shown graphically in Fig. 3. The elastic scattering cross section values computed using NJOY and those computed using the multi-group implementation of the RSM can be seen to coincide.

5. Application of the multi-group RSM to the Mosteller benchmark

An effect on effective multiplication is the ultimate impact of the correct (or incorrect) representation of scattering cross sections and of the neutron energy distribution *after* the interaction with the lattice nucleus. In order to evaluate this effect, the Mosteller benchmark is solved with correct data, derived using the new multi-group RSM code, and with traditional data based on the application of the asymptotic model. In this work the Mosteller benchmark is solved using the DRAGON code (Marleau et al., 2010). In the following sub-sections, the DRAGON code is described briefly, and then the approach taken for the generation of the cross section data is outlined. The remainder of the section is a description of the benchmark and of the results obtained that compare the two approaches (multi-group RSM and asymptotic models, respectively).

5.1. The DRAGON lattice physics code

The DRAGON (version 4) code is used in this study. The lattice physics DRAGON code is able to simulate the neutron behavior of unit cells or fuel assemblies of nuclear reactors, in one, two and three dimensional geometries, by solving the neutron transport equation through a variety of approaches such as the Method Of Characteristics (MOC), Collision Probability (CP) method, and the discrete ordinates method. A most attractive feature DRAGON offers, with respect to this study, is the option to have the macroscopic cross sections read into the code using an input data stream that allows any energy group structure, per the user's choosing. The "MAC" module of the DRAGON code allows the user to directly input the multi-group macroscopic cross-sections data (transport, fission, scattering, etc) "by hand" for each modeled mixture.

5.2. Generating the cross-section data

NJOY calculations were performed for each nuclide being modeled and the necessary cross-section data were extracted from the NJOY output. In parallel, starting from partly NJOY-processed data, the multi-group RSM standalone code was used to generate scattering matrices for the entire energy range for heavy nuclides.

The data obtained using these two approaches were then selectively combined into a single database: the scattering matrices generated from the RSM calculation were incorporated into the database along with all of the other (non-elastic scattering matrices) cross section data generated using NJOY. The database was written in a format acceptable by DRAGON. All the data in the NJOY output that are necessary for the lattice physics calculation were taken into account. Thus, the cross-section data, including capture, total, absorption, fission, (n, 2n), (n, 3n), and scattering, and other parameters such as the fission spectrum and total neutrons released per fission were collected and incorporated into the database. The scattering cross-sections are tabulated in matrix form. The amount of data can be considerable. For example, in the case of ^{238}U, for the 6914 groups library used in all these calculations, the scattering cross-section data are contained in several dozen matrices. The final collected database, as a prepared DRAGON input deck, is about 700 megabytes in memory and over 11.4 million lines long.

5.3. Mosteller pin-cell Doppler benchmark

The use of correctly derived resonance scattering cross sections and transfer functions in modeling a given system is expected to make a difference in the predicted reactivity, or equivalently in the predicted effective multiplication factor. In order to evaluate the magnitude of such an effect, the Mosteller benchmark for an LWR pin-cell is modeled. The cases considered here are one in which the cell is fueled with UO_2, reactor-recycled mixed-oxide (MOX), and weapons-grade MOX, respectively. The impact of using the corrected RSM model is evaluated specifically via a quantification of the Doppler effect on reactivity. The pin-cell is modeled with a fuel region, a gap, and a cladding in three concentric rings within a square pitch. The cladding consists of natural zirconium; the gap is modeled as a void; the coolant/moderator is borated water with a boron concentration of 1400 ppm. The fuel contained in the UOX pin-cell model included either two or three heavy isotopes (^{238}U, ^{234}U, and ^{235}U) and oxygen (^{16}O). In order to ensure spatial convergence 13 radial subdivisions in the fuel region and 4 Cartesian subdivision each along the x- and y-axis were specified in the DRAGON model. The benchmark evaluates the Doppler

Table 3
Fuel temperature coefficients for the Mosteller UOX benchmark with uranium enrichments ranging from 0.711% to 5.0% and the RSM kernel applied for all the heavy nuclei.

wt (%)	k (RSM kernel for all uranium nuclei)			FTC diff (%)
	HZP	HFP	FTC	
0.711	0.6614576	0.6548296	−5.10	−8.63
1.6	0.9553133	0.9461702	−3.37	−9.27
2.4	1.0929570	1.0828640	−2.84	−9.56
3.1	1.1706380	1.1600910	−2.59	−9.70
3.9	1.2330470	1.2221950	−2.40	−9.70
4.5	1.2683090	1.2573000	−2.30	−9.81
5.0	1.2925260	1.2814290	−2.23	−9.81

Table 4
Fuel temperature coefficients for the Mosteller Reactor-Recycle MOX fuel benchmark with 1–8 wt.% PuO_2 and the RSM kernel applied to all the heavy nuclei.

MOX composition (PuO_2 wt.%)	k (asymptotic kernel)			k (RSM kernel)			FTC diff. (%)
	HZP	HFP	FTC	HZP	HFP	FTC	
1.0	0.9407429	0.9312128	−3.63	0.9395729	0.9292448	−3.94	−8.74
2.0	1.0183990	1.0076460	−3.49	1.0171230	1.0055030	−3.79	−8.43
4.0	1.0759170	1.0644960	−3.32	1.0746340	1.0623330	−3.59	−8.05
6.0	1.1057560	1.0942010	−3.18	1.1045310	1.0921170	−3.43	−7.76
8.0	1.1297120	1.1181500	−3.05	1.1285580	1.1161660	−3.28	−7.48

Table 5
Fuel temperature coefficients for the Mosteller Weapons-Grade MOX fuel benchmark with 1–6 wt.% PuO_2 and the RSM kernel applied to all the heavy nuclei.

MOX composition (PuO_2 wt.%)	k (asymptotic kernel)			k (RSM kernel)			FTC diff. (%)
	HZP	HFP	FTC	HZP	HFP	FTC	
1.0	1.0838630	1.0748170	−2.59	1.0827770	1.0728730	−2.84	−9.79
2.0	1.1765110	1.1656680	−2.64	1.1753040	1.1635420	−2.87	−8.79
4.0	1.2472990	1.2352440	−2.61	1.2460520	1.2330640	−2.82	−8.04
6.0	1.2847710	1.2725020	−2.50	1.2835640	1.2703840	−2.69	−7.71

Table 6
Fuel temperature coefficients for the Mosteller Reactor-Recycle MOX fuel benchmark with 1–8 wt.% PuO_2 and the RSM kernel applied to ^{238}U only.

MOX composition (PuO_2 wt.%)	HZP	HFP	FTC	FTC diff. (%)
1.0	0.9398723	0.9296191	−3.91	−7.87
2.0	1.0175060	1.0059940	−3.75	−7.33
4.0	1.0750620	1.0628910	−3.55	−6.81
6.0	1.1049570	1.0926810	−3.39	−6.46
8.0	1.1289670	1.1167140	−3.24	−6.18

Table 7
Fuel temperature coefficients for the Mosteller Weapons-Grade MOX fuel benchmark with 1–6 wt.% PuO_2 and the RSM kernel applied to ^{238}U only.

MOX composition (PuO_2 wt.%)	HZP	HFP	FTC	FTC diff. (%)
1.0	1.0828870	1.0730010	−2.84	−9.57
2.0	1.1755180	1.1637980	−2.86	−8.35
4.0	1.2463530	1.2334410	−2.80	−7.35
6.0	1.2838850	1.2707980	−2.67	−6.88

coefficients of reactivity for seven different ^{235}U enrichment cases each at two temperatures, thus quantifying the feedback from Hot Zero Power (HZP) at 600 K to Hot Full Power (HFP) at 900 K. The fuel temperature coefficient (FTC) in units of pcm/K is calculated using

$$FTC = \left(\frac{1}{k_{HZP}} - \frac{1}{k_{HFP}}\right)\frac{1\times 10^5}{\Delta T} \quad (8)$$

where k_{HZP} is the eigenvalue (effective multiplication factor) at Hot Zero Power (600 K), k_{HZP} is the eigenvalue at Hot Full Power (900 K) and ΔT is the change in temperature. The pin-cell was analyzed using the DRAGON code for both the asymptotic model and the resonance scattering model. The cross-section data are obtained using NJOY complemented with the standalone RSM model.

5.4. UOX pin-cell model

Tables 2 and 3 summarize the results for the Doppler coefficients by first applying the corrected scattering model to the ^{238}U isotope only and then to the remaining uranium isotopes (^{234}U, ^{235}U)[2] as well. The results displayed in Tables 2 and 3 show less than a 0.1% change in the fuel temperature coefficient when applying the RSM to all heavy nuclei as opposed to only ^{238}U. It is clear that the contribution of neutron up-scattering due to nuclei other than ^{238}U (^{235}U, ^{234}U) in the UOX benchmark is negligible at all the enrichment levels considered in these tables (up to 5%).

5.5. MOX pin-cell model

Calculations were also performed for the second and third subsets of the Mosteller benchmark, which pertain to MOX fuel. These two subsets contain reactor-recycle MOX fuel with 1–8 wt.% PuO_2 (i.e., recycled reactor-grade MOX) and weapons grade MOX with 1–6 wt.% PuO_2, respectively. The Doppler coefficients were calculated for the situations at HZP (600 K) and at HFP (900 K), and the results are shown in Tables 4 and 5.

In both MOX cases the corrected resonance scattering model, when applied to all heavy nuclei, is responsible for a drop in the fuel temperature coefficient in the range of 7.48–9.79%. Further calculations were carried out to ascertain the up-scattering contributions by all the individual nuclei modeled in the MOX case and their respective influences on the eigenvalues. Calculations first applied the corrected resonance scattering model solely to ^{238}U for both MOX cases. Those results are displayed in Tables 6 and 7.

The results when applying the corrected scattering model to all nuclei and then only for ^{238}U account for a FTC difference by as much as 1.3%. In the case of 8 wt.% PuO_2 of the reactor-recycle MOX fuel, for example; applying RSM for ^{238}U as opposed to all heavy nuclides is responsible for a drop of 1.3% in the FTC difference. Of the −7.48% FTC difference, 83% is due to ^{238}U, 5.0% is attributable to ^{242}Pu and 10% to ^{240}Pu. The balance (2%) is attributable to the remaining nuclides.

[2] The 0.711 $^{wt}/_{o}$ enrichment case was modeled without the ^{234}U isotope as specified by the benchmark.

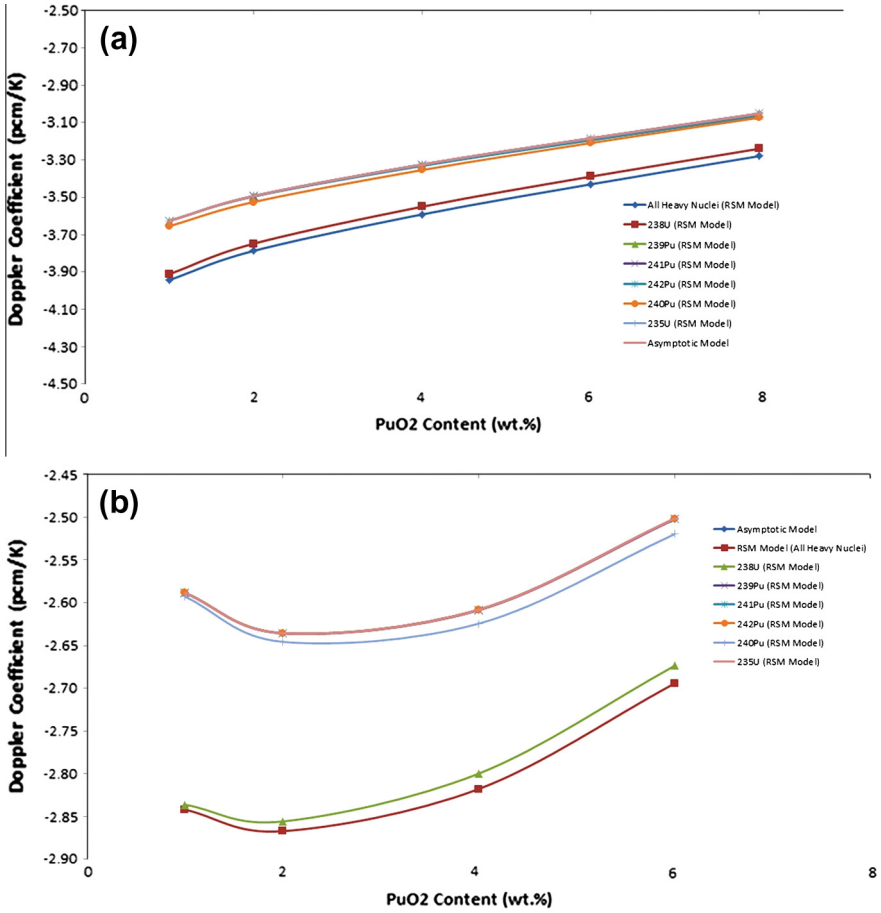

Fig. 4. Fuel temperature coefficient for the (a) Reactor-Recycle MOX fuel pin and (b) Weapons-Grade MOX fuel pin when applying the RSM to individual nuclei.

Table 8
The up-scattering percentage contribution of each nucleus towards the eigenvalue for Mosteller Reactor-Recycle MOX fuel benchmark with 1–8 wt.% PuO_2 at 600 K.

MOX composition (PuO_2 wt.%)	^{238}U	^{235}U	^{239}Pu	^{240}Pu	^{241}Pu	^{242}Pu
1.0	74.51	0.09	0.04	2.59	22.58	0.19
2.0	70.15	0.16	0.08	6.13	23.33	0.16
4.0	66.85	0.39	0.23	11.65	20.72	0.16
6.0	65.60	0.49	0.33	15.19	18.23	0.16
8.0	64.84	0.78	0.52	17.75	15.93	0.17

Table 9
The up-scattering percentage contribution of each nucleus towards the eigenvalue for Mosteller Reactor-Recycle MOX fuel benchmark with 1–8 wt.% PuO_2 at 900 K.

MOX composition (PuO_2 wt.%)	^{238}U	^{235}U	^{239}Pu	^{240}Pu	^{241}Pu	^{242}Pu
1.0	81.17	0.07	0.03	1.65	16.95	0.14
2.0	77.30	0.14	0.09	4.07	18.25	0.14
4.0	74.62	0.28	0.14	8.00	16.83	0.14
6.0	73.54	0.39	0.24	10.64	15.05	0.15
8.0	73.12	0.56	0.31	12.53	13.39	0.10

More calculations were carried out in which the new resonance scattering formulation is applied to each heavy nucleus individually (^{238}U, ^{235}U, ^{239}Pu, ^{241}Pu, ^{242}Pu, ^{240}Pu). A plot of the results showing the Doppler coefficient for each case when each nuclide is considered on an individual basis is presented in Fig. 4. Using the corresponding computational results, the contribution of each nucleus responsible for a change in the fuel temperature coefficient, when comparing the asymptotic and resonance scattering kernels, is calculated. Those results are summarized in four tables

Table 10
The up-scattering percentage contribution of each nucleus towards the eigenvalue for Mosteller Weapons-Grade MOX fuel benchmark with 1–6 wt.% PuO_2 at 600 K.

MOX composition (PuO_2 wt.%)	^{238}U	^{235}U	^{239}Pu	^{240}Pu	^{241}Pu	^{242}Pu
1.0	89.87	0.18	0.00	0.00	9.76	0.18
2.0	82.41	0.33	0.00	0.00	17.10	0.17
4.0	75.98	0.64	0.00	0.00	23.21	0.16
6.0	73.59	0.91	0.00	0.00	25.33	0.17

Table 11
The up-scattering percentage contribution of each nucleus towards the eigenvalue for Mosteller Weapons-Grade MOX fuel benchmark with 1–6 wt.% PuO_2 at 900 K.

MOX composition (PuO_2 wt.%)	^{238}U	^{235}U	^{239}Pu	^{240}Pu	^{241}Pu	^{242}Pu
1.0	93.51	0.15	0.00	0.00	6.18	0.15
2.0	88.08	0.28	0.00	0.00	11.49	0.14
4.0	82.90	0.51	0.00	0.00	16.46	0.14
6.0	80.80	0.71	0.00	0.00	18.40	0.09

(Tables 8–11) and show the contribution of up-scattering from nuclei other than ^{238}U is non-negligible.

5.6. Effect of resonance scattering model on the flux energy dependence

Near pronounced scattering resonances the correct treatment of the cross sections, which incorporates lattice vibration effects, gives rise to substantial amounts of up-scattering. The consequence is a local change in the energy dependence of the neutron

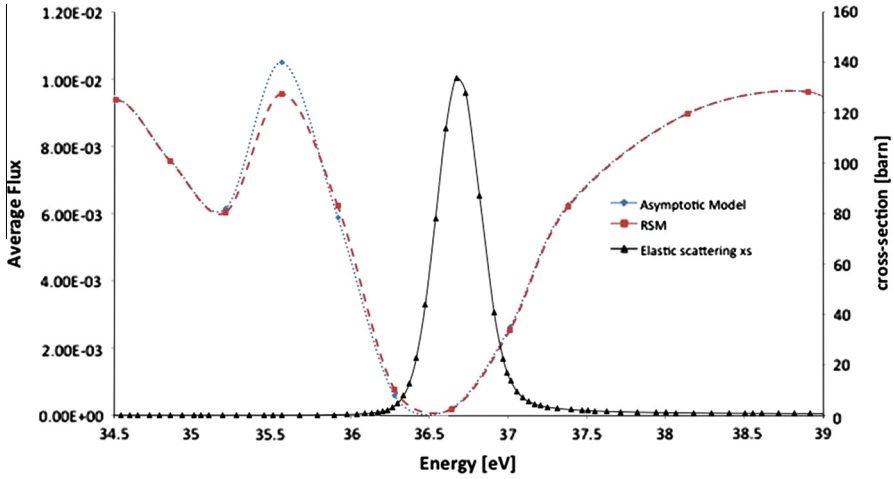

Fig. 5. Neutron flux of the fuel region for UO_2 pin-cell at 0.711 wt.% enrichment at 600 K near the third resonances of ^{238}U, 36.68 eV, using the RSM (dashed curve) and the traditional asymptotic (dotted curve) model. The elastic scattering cross section is also plotted (solid curve).

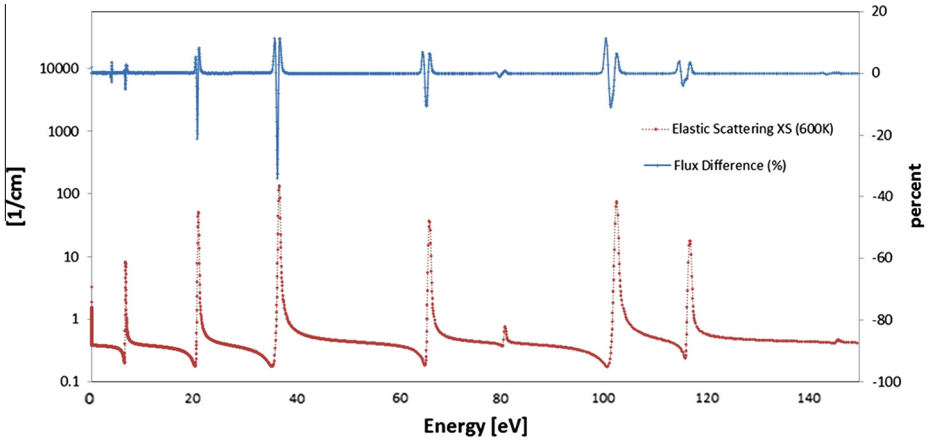

Fig. 6. Relative difference in flux (%, solid curve above) between the asymptotic model and the resonance scattering model plotted against the macroscopic cross-section of the fuel (dotted curve below). Where the flux is almost zero, the relative error is very large (which cannot be seen in Fig. 5 due to the scale in that figure).

flux, i.e., a change in the neutron spectrum. For example, a major visible difference seen in the flux occurs near the 36.68 eV scattering resonance in ^{238}U (Fig. 5). The flux computed with the corrected scattering model deviates from the flux obtained using the asymptotic model by a relative difference of −11.22% at 35.79 eV. In the same pin-cell study as the one of the results just discussed, but at HFP conditions (900 K), the correct flux peak at the same energy region differs by −14.27% from the asymptotic kernel-based flux. These numbers are almost the same independent of the uranium enrichment (up to the higher range of the low enrichment levels discussed in this paper). The MOX fuel benchmarks also displays similar results at 35.79 eV. As intuitively expected, the greatest change in flux shape is observed at energies that correspond to where the elastic cross-section is largest (Fig. 6).

6. Summary of results and conclusion

The temperature-dependent resonance scattering formula takes into account the thermal agitation of the host medium and predicts the occurrence of up-scattering effects in the slowing down domain that are, thus, no longer neglected. This is a significant departure from the practice that stems from the traditional use of the simplified asymptotic model. The formulation presented here, and its implementation, make possible the assessment of the effect of the correct treatment of lattice motion (i.e., this new model) on deterministic reactor core analyses, whereas implementations by others were thus far confined to Monte Carlo codes. The applications presented here, though limited to cell-level situations, demonstrate the impact of the use of the RSM.

The results shown in the previous subsections demonstrate that the asymptotic model used to describe neutron-nuclei elastic scattering leads to almost 10% under prediction of the Doppler coefficients for LWR lattices of UO_2 and MOX fuels. In the case of the UO_2 fuel, the contribution of up-scattering was overwhelmingly due to ^{238}U. The change in Doppler coefficients decreases slightly with enrichment. When using the RSM instead of the asymptotic model, and for each temperature, in the cases of UO_2 fuel, the change in eigvenvalues ranges from 68 to 208 pcm. Furthermore, this study also showed that applying RSM to the ^{235}U and ^{234}U nuclei, at the same given conditions (up to 5 $^{w}/_{o}$ ^{235}U), results in a negligible impact: a difference of at most 2 pcm in eigenvalues and less than 0.1% difference in the Doppler coefficient between the RSM and the asymptotic scattering model results.

As for the MOX cases, the asymptotic scattering model leads to an under prediction by 8–10% for the case of the weapons-grade MOX fuel and 7–9% for the reactor-recycled MOX fuel. The change in eigenvalues for each calculation at HZP and HFP ranges from 115 to 216 pcm for the reactor-recycle MOX fuels and from 109 to

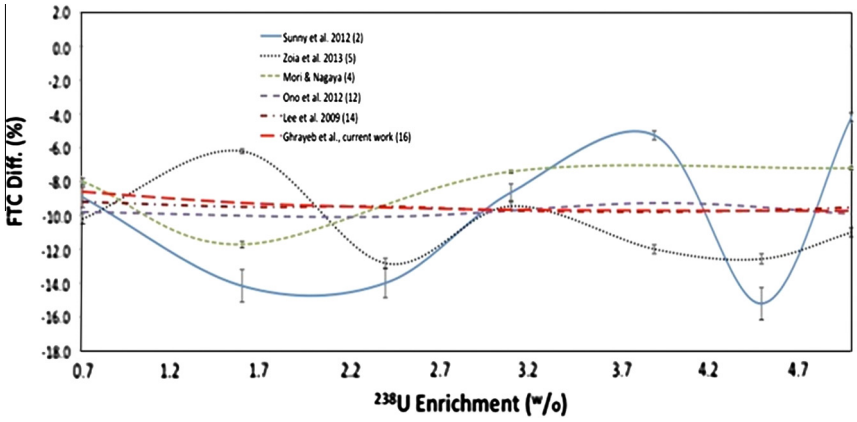

Fig. 7. Comparison of the FTC differences for UOX Mosteller benchmark. The results of Ghrayeb et al. (long dashed curve) and Lee et al. 2009 (dash dot curve) compare relatively well against each other showing a nearly constant behavior in FTC difference with respect to ^{235}U enrichment. However, there is no consensus among the work of others to show consistency in FTC difference with respect to ^{235}U enrichment. The numbers in parentheses correspond to the first column of Table 1.

218 pcm for the weapons-grade MOX fuel. Furthermore, in these cases, nuclei other than ^{238}U were responsible for as much as 1.3% change in the Doppler coefficients. The ^{241}Pu nuclei contribute as much as 23% (depending on the PuO_2 composition) for the Reactor-Recycle MOX fuel followed by ^{240}Pu, which contributes almost 18% in certain cases. The ^{239}Pu and ^{242}Pu nuclei contribute less than 1% of the up-scattering. In the case of the weapons-grade MOX fuel the largest and most significant contribution to resonance up-scattering after that of ^{238}U is that of ^{241}Pu, which is responsible for as much as 25% of up-scattering. Unlike in the case of the reactor-recycle MOX fuel, ^{240}Pu does not contribute at all to resonance scattering for weapons-grade MOX. This is most likely due to the fact that there is as much as five times more ^{240}Pu in the reactor-recycle MOX isotopic distribution than in that of the weapons-grade MOX.

In Section 2, a brief history of the application of the RSM model and a snapshot of current developments were presented. In particular, Table 1 was provided that summarizes the results of the application of the RSM to the Mosteller benchmarks by various authors. Those results are displayed graphically in Fig. 7. The most remarkable feature in this figure is that the deterministic implementation of Ghrayeb and co-workers and that of Lee and co-workers give very similar results in magnitude and trend as enrichment is increased from 0.711% to 5%. The results of Ono and co-workers are also close to the ones just cited, albeit it with some noticeable difference and a different trend. In contrast, the Monte Carlo implementations give very different results from the deterministic implementations and, more surprisingly, from one another. Although most of the authors of the Monte Carlo-based results stated that theirs were in "good agreement" with those of others, the figure shows that in fact, even when the reported errors are accounted for, the various Monte Carlo results appear to be in contradiction. The error bars shown in the figure are plotted from the reported errors in the various cited publications. As can be seen, only one pair of error bars displays any level of overlap. The figure actually shows that the Monte Carlo results do not even follow the same trend as enrichment varies. The figure shows that the Monte Carlo results need to be reconciled with one another and with the deterministic ones. It is beyond the scope of the present paper to find an explanation for the observed discrepancies; however, it is easy to speculate that perhaps the Monte Carlo results are simply not converged during the scattering kernel evaluation. However, that speculation seems to be contradicted by the very narrow error bands implied in the reporting by the various authors.

For the sake of completeness, it is important to mention results by others that are not listed in Table 1 and not represented in Fig. 7. Specifically, Trumbull and Fieno reported that they also modeled the UOX Mosteller benchmark. Their results were not explicitly documented in their paper, but they reported that they obtained "excellent agreement to previously documented results for MCNP5 (Sunny et al., 2012) and MVP (Mori and Nagaya, 2009)". However, as stated previously and as shown in Fig. 7 the various FTC difference Monte Carlo results do not seem to follow any trend and the results from the various authors seem different from one another, including those of Sunny et al. 2012 and those of Mori and Nagaya 2009.

Acknowledgements

This research was performed in part using funding received from the US Department of Energy Office of Nuclear Energy's Nuclear Energy University Programs. Some financial support was received from the Deep Burn Project (Coated Particles Fuel element of the Department of Energy Fuels campaign). Both sources of support are gratefully acknowledged.

References

Arbanas, G., et al., 2011. Computation of temperature-dependent Legendre moments of a double-differential elastic cross section. In: Proceedings of International Conference on Mathematics and Computational Methods Applied to Nuclear Science and Engineering, (Rio de Janeiro, Brazil), May 8–12, 2011.

Arbanas, G., et al. 2012. Convergence of Legendre expansion of Doppler-broadened double-differential elastic scattering cross section. PHYSOR 2012 – Advances in Reactors Physics Linking Research, Industry and Education (Knoxville, TN, USA), April 15–20, 2012.

Becker, B., 2010. Doctorate Thesis. "On the influence of the resonance scattering treatment in Monte Carlo codes on High Temperature Reactor characteristic", Institut für Kernenergetik und Energiesysteme, University of Stuttgart, Germany.

Becker, B., Dagan, R., Broedres, C.H.M., Lohnert, G.H., 2009a. Improvement of the resonance scattering treatment in MCNP in view of HTR calculations,. Annals of Nuclear Energy 36, 281–285.

Becker, B., Dagan, R., Lohnert, G., 2009b. Proof and implementation of the stochastic formula for ideal gas, energy dependent scattering kernel. Annals of Nuclear Energy 36, 470–474.

Becker, B., Dagan, R, Broeders, C. H. M., Lohnert, G., 2009c. An alternative stochastic Doppler broadening algorithm. In: International Conference on Mathematics, Computational Methods & Reactor Physics, (Saratoga Spring, New York), May 3–7, 2009.

Becker, B., Dagan, R., Broeders, C. H. M., Lohnert, G. H., 2008. Improvement of the resonance scattering treatment in MCNP in view of HTR calculations. In: International Conference on the Physics of Reactors "Nuclear Power: A Sustainable Resource" (Interlaken, Switzerland), September 14–19, 2008.

Blackshaw, B.L., Murray, R.L., 1967. Scattering functions for low-energy neutron collisions in a Maxwellian monatomic gas. Nuclear Science and Engineering 27, 520–532.

Bouland, O., Kolesov, V., Rownalds, J.L., 1994. The effect of approximations in the energy distributions of scattered neutrons on thermal reactor Doppler effects. In: Int. Conf. on Nuclear Data for Science and Technology, (Gatlinburg, Tennessee, USA), May 9–13, 1994, pp. 1006–1008.

Cuello, G.J., Granada, J.R., 1997. Thermal neutron scattering by Debye solids: a synthetic scattering function. Annals of Nuclear Energy 24 (10), 763–783.

Courcelle, A. and Rowlands, J., 2007. Approximate model of neutron resonant scattering in a crystal, unpublished.

Cullen, D.E., Weisbin, C.R., 1976. Exact Doppler broadening of tabulated cross sections. Nuclear Science and Engineering 60, 199–229.

Dagan, R., Becker, B., Roubtsov, D., 2011a. Evaluation of the CANDU 6 neutron characteristics in view of application of the resonance dependent scattering kernel in MCNP(X). Nuclear Science and Technology 2, 782–787.

Dagan, R. et al., 2011b. Modelling a resonance dependent angular distribution via DBRC in Monte Carlo Codes. Journal of the Korean Physical Society 59 (2), 983–986.

Dagan, R., Rowlands, J., Courcelle, A., Lubitz, C. R., 2007. On the treatment of neutron scattering in the resonance range. In: International Conference on Nuclear Data for Science and Technology, (Nice, France), April 22–27, 2007.

Dagan, R., Broeders, C.H.M. 2006. On the effect of resonance dependent scattering-kernel on fuel cycle and inventory, in: PHYSOR 2006, ANS Topical Meeting on Reactor Physics, (Vancouver, BC, Canada), September 10–14 2006.

Dagan, R., 2005. On the use of $S(\alpha, \beta)$ tables for nuclides with well pronounced resonances. Annals of Nuclear Energy 32, 367–377.

Dagan, R., 2004. On the importance of a new formula for the double differential scattering kernel, in PHYSOR 2004 – The Physics of Fuel Cycles and Advanced Nuclear Systems: GlobalDevelopments, (Chicago, IL, USA), April 25–29, 2004.

Danon, Y. et al., 2009. Benchmarking experiment of neutron resonance scattering models in Monte Carlo codes. In: International Conference on mathematics, Computational Methods & Reactor Physics, M&C 2009, (Saratoga Springs, NY, USA), May 3–7, 2009.

Ghrayeb, S.Z. 2013. Doctorate Thesis. Deterministic multigroup modeling of thermal effect on neutron scattering by heavy nuclides, Pennsylvania State University, PA, USA.

Ghrayeb, S.Z., Ouisloumen, M., Ougouag, A.M. Ivanov, K.N., 2012. Multi-group computation of the temperature-dependent resonance scattering model (RSM) and its implementation, in PHYSOR – Advances in Reactor Physics – Linking Research, Industry, and Education, (Knoxville, TN), April 15–20, 2012.

Ghrayeb, S.Z., Ouisloumen, M., Ougouag, A.M., Ivanov, K.N., 2011a. Computation of the resonant neutron scattering to higher angular moments. Trans. Am. Nucl. Soc., vol. 105, October 30 –November 3, 2011. Invited paper.

Ghrayeb, S.Z., Ouisloumen, M., Ougouag, A.M., Ivanov, K.N., 2011b. Deterministic modeling of higher angular moments of resonant neutron scattering. Annals of Nuclear Energy 38, 2291–2297.

Ghrayeb, S.Z., Ouisloumen, M., Ougouag, A.M., Ivanov, K.N., 2011c. Multi-group formulation of the resonance scattering model (RSM) and its implementation. In: International Conference on Physics and Technology of Reactors and Applications, (Fez, Morocco), September 26–28, 2011.

Ghrayeb, S.Z., Ouisloumen, M., Ougouag, A.M., Ivanov, K.N., 2010a. The resonance neutron scattering angular moments using the deterministic approach. Trans. Am. Nucl. Soc. 103.

Ghrayeb, S.Z., Ouisloumen, M., Ougouag, A.M., Ivanov, K.N., 2010b. Effect of the resonance scattering model on reactor core calculations. In: Proceedings of High Temperature Reactors, (Prague, Czech Republic), October 18–20, 2010.

Grandi, G., Smith, K., Xu, Z., Rhodes, J., 2010. Effect of CASMO-5 cross-section data and Doppler temperature definitions on LWR reactivity initiated accidents. In: International Conference on Reactor Physics – Advanced in Reactor Physics to Power the Nuclear Renaissance, (Pittsburgh, PA USA), May 9–14, 2010.

Hart, S.W.D., Maldonado, G.I., Goluoglu, S., Rearden, B., 2013. Implementation of the Doppler broadening rejection correction in KENO. Trans. Am. Nucl. Soc 108.

Hove, L.V., 1954. Correlations in space and time and Born approximation scattering in systems of interacting particles. Physical Review 95 (1), 249–262.

Kim, Y., Hartanto, D., 2012. A high-fidelity Monte Carlo evaluation of CANDU-6 safety parameters. In: International Conference on Reactor Physics, Linking Research, Industry and Education, (Knoxville, TN, USA), April 15–20, 2012.

Kolesov, V.V., Ukrainstev, V.F., 2006. Temperature effects and resonance elastic cross section influence on secondary energy distributions of scattered neutrons in the resolved resonance region, in ANS Topical Meeting on Reactor Physics, (Vancouver, British Columbia, Canada), September 10–14 2006.

Kurchenkov, A.Yu., Laletin, N.I., 1991. Neutron-scattering indices at moving monoatomic-gas nuclei. Atomnaya Énergiya 70 (6), 368–372.

Lamb Jr., W.E., 1939. Capture of neutrons by atoms in a crystal. Physical Review 55, 190–197.

Lee, D., Smith, K., Rhodes, J., 2009. The impact of ^{238}U resonance elastic scattering approximations on thermal reactor Doppler reactivity. Annals of Nuclear Energy 36, 274–280.

Lee, D., Smith, K., Rhodes, J., 2008. The impact of ^{238}U resonance elastic scattering approximations on thermal reactor Doppler reactivity. In: International Conference on Reactor Physics, Nuclear Power: A sustainable Resource, (Interlaken, Switzerland), September 14–19, 2008.

MacFarlane, R.E., Muir, D.W., 2000. NJOY 99.0 code System for Producing Pointwise and Multigroup neutron and Photon Cross Sections from ENDF/B Data, Los Alamos National Laboratory, Los Alamos, NM.

Marleau, G., Hébert, A., Roy, R., 2010. A User Guide for Dragon Version4, Technical Report IGE 294, École Polytechniquue de Montréal, 2010.

Meister, A., Santamarina, A., 1998. The effective temperature for Doppler broadening of neutrons resonances in UO2, in International Conference on the Physics of Nuclear Science and Technology, (Long Island, NY, USA), vol. 1, October 5–8, 1998, pp. 233–239.

Mori, T., Nagaya, Y., 2009. Comparison of resonance elastic scattering models newly implemented in MVP continuous-energy monte carlo code. Journal of Nuclear Science andTechnology 46 (8), 793–798.

Mosteller, R. D. 2006. Computational benchmark for the Doppler reactivity defect, Tech. Rep. LA-UR-06-2968, Los Alamos National Laboratory, 2006.

Mosteller, R. D. 2007. ENDF/B-V, ENDF/B-VI, and ENDF/B-VII.0 results for the Doppler-defect benchmark, in Joint International Topical Meeting on Mathematics and Computation and Supercomputing in Nuclear Applications, (Monterey, CA), April 15–19, 2007.

Naberejnev, D., Mounier, C., Sanchez, R., 1999. The influence of crystalline binding on resonant absorption and reaction rates. Nucl. Sci. & Eng. 131, 222–229.

Naberejnev, D.G., 2001. A model that takes into account the influence of chemical binding on neutron scattering in a resonance. Annals of Nuclear Energy 28, 1–24.

Nagaya, Y., et al., 2005. MVP/GMVP II: General-Purpose Monte Carlo Codes for Neutron and Photo Transport Calculations based on Continuous Energy and Multigroup Methods. JAEI-1348 Japan Atomic energy Research Institute.

Oberle, P. 2010. Doctorate thesis, Application of a new resonance formalism to Pressurized Water Reactors, Institut für Kernenergetik und Energiesysteme, University of Stuttgart, Germany.

Ono, M., Wada, K., Kitada, T., 2012. Simplified treatment of exact resonance elastic scattering model in deterministic slowing down equation, in PHYSOR 2012 – Advances in Reactor Physics –Linking Research, Industry, and Education, (Knoxville, TN, USA) April 15–20, 2012.

Ouisloumen, M., Sanchez, R., 1990. A model for neutron scattering off heavy isotopes that accounts for thermal agitation effects. Nuclear Science and Engineering 107, 189–200.

Ouisloumen, M. 1989. Contribution aux dévéloppements du code de transport APOLLO-II: Noyau de l'opérateur de ralentissement tenant compte de l'agitation thermique; effet des resonances sur les transferts en energie, Doctorate Thesis, Université de Paris-Sud (in French), Marc 1989.

Peng, S., Zhang, S., Jiang, Z., 2010. Investigations on the impact of heavy nuclides resonance elastic scattering models on resonance integrals. In: Proceedings of the 18th International Conference on Nuclear Engineering, ICONE 18, (Xi'an, China), May 17–21, 2010.

Rhodes, J., Smith, K., Lee, D., 2006. CASMO-5 development and applications, in Advances in Nuclear Analysis and Simulation, PHYSOR 2006, (Vancouver, BC, Canada), September 10–14, 2006.

Ro, T-I, Danon, Y., Liu, E., Barry, D.P., Dagan, R., 2009. Measurements of the neutron scattering spectrum from ^{238}U and comparison of the results with a calculation at the 36.68-eV resonance. Journal of the Korean Physical Society 55 (4), 1389–1393.

Rothenstein, W., 2004. Proof of the formula for the ideal gas scattering kernel for nuclides with strongly energy dependent scattering cross section. Annals of Nuclear Energy 31, 9–23.

Rothenstein, W., Dagan, R., 1998. Ideal gas scattering kernel for energy dependent cross-sections. Annals of Nuclear Energy 25 (45), 209–222.

Rothenstein, W., 1996. Neutron scattering kernels in pronounced resonances for stochastic Doppler effect calculations. Annals of Nuclear Energy 23 (4/5), 441–458.

Rothenstein, W., Dagan, R., 1995. Two-body kinetics treatment for neutron scattering from a heavy Maxwellian gas. Annals of Nuclear Energy 22 (11), 723–730.

RSICC Computer Code Collection, CCC_732, 2011. Scale: A Comprehensive Modeling and Simulation Suite for Nuclear Safety Analysis and Design. Technical Report ORNL/TM-2005/39, Version 6.1, Oak Ridge National Laboratory.

Sanchez, R., Hewko, C., Santandrea, S., 2013. Numerical computation of Doppler-broadening in the resonance domain. In: International Conference on Mathematics and Computational Methods Applied to Nuclear Science and Engineering, (Sun Valley, Idaho, USA), May 5–9, 2013.

Sanchez, R., et al. 1988. APOLLO II: a user-oriented, portable, modular code for multigroup transport assembly calculations. Nuclear Science and Engineering 100.

Sunny, E.E., 2013. Doctorate Thesis, On-the-fly generation of differential resonance scattering probability distribution functions for Monte Carlo Codes, University of Michigan, 2013.

Sunny, E., Martin, W., 2013. On-the-fly generation of differential resonance scattering probability distribution functions for Monte Carlo codes. In: International Conference on Mathematics and Computational Methods Applied to Nuclear Science & Engineering, M&C 2013 (Sun Valley, Idaho, USA), May 5–9, 2013.

Sunny, E.E., Brown, F.B., Kiedrowski, B.C., Martin, W.R., 2012. Temperature effects of resonance scattering for epithermal neutrons in MCNP, in PHYSOR 2012 – Advances in Reactor Physics – Linking Research, Industry, and Education, (Knoxville, TN, USA), April 15–20, 2012.

Sutton, T. M., et al., 2007. The MC21 Monte Carlo Code. In: Proceedings International Conference on Mathematics & Computations andSupercomputing in Nuclear Applications (Monterey, CA, USA), April 15–19, 2007.

Trumbull, T.H., Fieno, T., 2013. Effects of applying the Doppler broadened rejection correction method for LEU and MOX pin-cell depletion calculations. Annals of Nuclear Energy 62, 184–194.

Wigner, E.P., Wilkins, J.E. Jr., 1944. Effect of the temperature of the moderator on the velocity distribution of neutrons with numerical calculations for H as moderator, Technical Report AECD -2275, Oak Ridge National Laboratory, Oak Ridge, Tennessee, September 14, 1944.

Word, R.E., Trammell, G.T., 1981. Investigation of condensed matter via resonant neutron scattering. Correlation-function formalism with application to the study of the interatomic force density. Physical Review B 24 (5), 2430–2448.

X-5 Monte Carlo Team, 2003. MCNP – A General Carlo N-Particle Transport Code, Version 5, Volume 1: overview and theory. LA-UR-03-1987, Los Alamos Laboratory.

Zoia, A., Brun, E., Jouanne, C., Malvagi, F., 2013. Doppler broadening of neutron elastic scattering kernel in TRIPOLI-4. Annals of Nuclear Energy 54, 218–226.